Biopharmaceutical Characterization and Stability of Nabumetone–Cyclodextrins Complexes Prepared by Grinding

David Klarić [1], Željka Soldin [1], Anna Vincze [2,3], Rita Szolláth [2,3], György Tibor Balogh [2,3], Mario Jug [4,*] and Nives Galić [1,*]

[1] Department of Chemistry, Faculty of Science, University of Zagreb, Horvatovac 102a, 10 000 Zagreb, Croatia
[2] Department of Pharmaceutical Chemistry, Semmelweis University, Hőgyes Endre u. 9., H-1092 Budapest, Hungary
[3] Center for Pharmacology and Drug Research & Development, Semmelweis University, Üllői u. 26. H-1092 Budapest, Hungary
[4] Department of Pharmaceutical Technology, Faculty of Pharmacy and Biochemistry, University of Zagreb, A. Kovačića 1, 10 000 Zagreb, Croatia

Supporting Information

Contents

1. Materials and methods 2
2. Characterization of NAB complexes in solid state 3
2.1. DSC and XRPD 3
2.2. FT IR spectroscopy 6
3. Effect of β-cyclodextrins on NAB chemical and photochemical stability 11
3.1. Hydrolytic degradation 11
3.2. Photostability study 19
3.3. Long-term stability study 21

1. Materials and methods

Table S1. Chromatographic parameters for stability-indicating UHPLC-DAD and UHPLC-HRMS methods.

Parameter	Developed LC method		
Column	Agilent ZORBAX RRHD Eclipse Plus C18		
Mobile phase A (MF_A)	0.1 % (*v*/*v*) formic acid in water		
Mobile phase B (MF_B)	0.1 % (*v*/*v*) formic acid in methanol		
Gradient elution profile	Time / min	MF_A / %	MF_B / %
	0	95	5
	15	5	95
Injection volume (UHPLC-HRMS)	1 µL		
Injection volume (UHPLC-DAD)	2 µL		
Mobile phase flow	0.20 mL/min		
Column temperature	40 °C		
Detection (DAD)	231, 254, 260, 266, and 275 nm		
Detection (MS)	ESI+ (100 – 1300 *m*/*z*)		

Table S2. Instrument parameters for acquiring total ion chromatograms, TICs.

Parameter	Value
Sheath gas temperature	250 °C
Sheath gas flow	11 L/min
Nebulizer pressure	25 psi
Capillary voltage	2500 V
Nozzle voltage	1000 V
Drying gas temperature	200 °C
Drying gas flow	17 L/min
Fragmentor voltage	100 V

2. Characterization of NAB complexes in solid state

2.1. DSC and PXRD

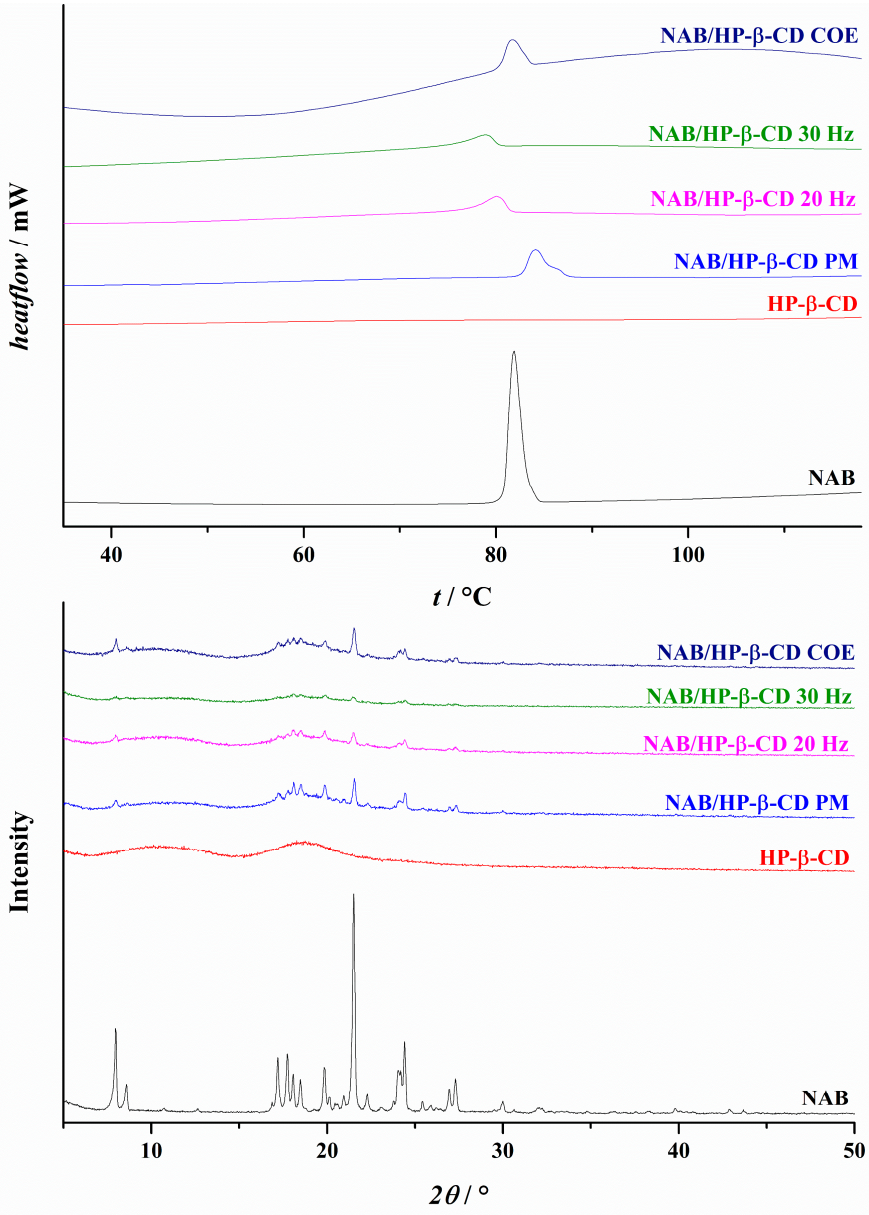


Figure S1. DSC thermograms (up) and PXRD diffractograms (down) of starting compounds (NAB and HP-β-CD), ground and co-evaporated drug (NAB GR and NAB COE), physical mixture (NAB/HP-β-CD PM), and complexes obtained by co-grinding (NAB/HP-β-CD GR) and co-evaporation (NAB/HP-β-CD COE).

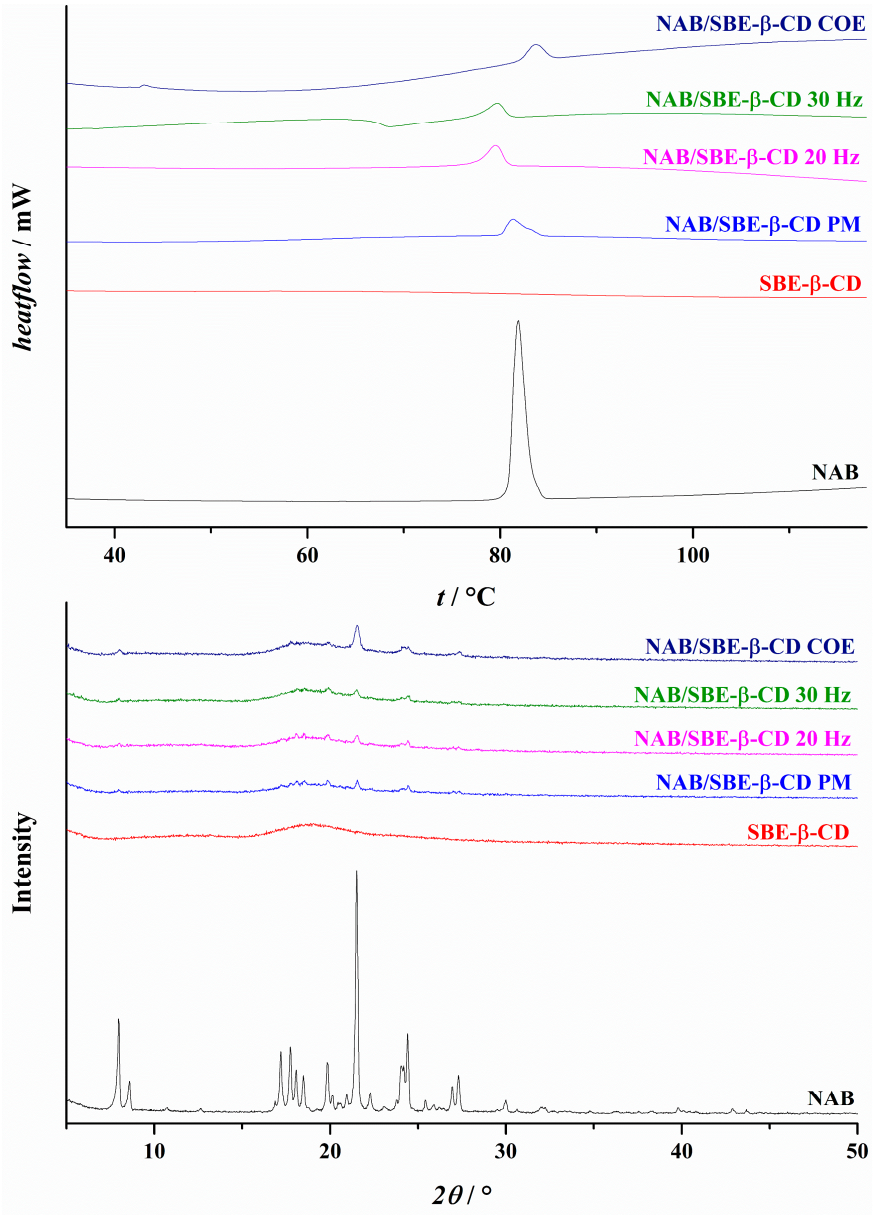


Figure S2. DSC thermograms (up) and PXRD diffractograms (down) of starting compounds (NAB and SBE-β-CD), ground and co-evaporated drug (NAB GR and NAB COE), physical mixture (NAB/SBE-β-CD PM), and complexes obtained by co-grinding (NAB/SBE-β-CD GR) and co-evaporation (NAB/SBE-β-CD COE).

Table S3. The effect of the processing parameters of the characteristics of the products obtained by co-grinding and co-evaporation: onset temperature (T_{onset}), peak temperature (T_{peak}), fusion enthalpy (ΔH_{fusion}) and residual drug crystallinity in the product (RDC) obtained by DSC analysis.

Sample	**Grinding time / (min)**	**Grinding frequency / (Hz)**	T_{onset} /(°C)	T_{peak} /(°C)	ΔH_{fusion} / (Jg^{-1})	**RDC / (%)**
NAB	0	20	80.9	81.9	139.0	100.0
	30		80.7	81.7	137.3	98.8
	60		81.8	82.9	132.6	95.4
	90		80.6	81.9	141.6	101.8
	120		82.4	83.7	126.4	90.9
	NAB COE		84.2	85.8	131.9	95.1
NAB/β-CD	0	20	81.6	83.4	120.5	88.5
	30		79.1	80.9	111.6	82.0
	60		78.8	80.6	99.4	73.1
	90		77.9	80.4	97.7	71.8
	120		76.7	79.9	92.3	67.8
	NAB/β-CD COE		80.5	81.7	36.9	26.6
NAB/HP-β-CD	0	20	82.7	84.1	136.3	100.2
	30		79.8	81.7	123.3	90.7
	60		79.1	81.3	123.9	91.1
	90		80.2	82.7	110.6	81.3
	120		77.1	80.0	102.2	75.1
	0	30	82.7	84.1	136.3	101.4
	30		78.1	80.2	113.2	84.2
	60		77.7	80.4	91.3	67.9
	90		75.4	78.9	66.1	49.2
	120		-	-	-	0
	NAB/HP-β-CD COE		80.3	81.7	134.5	96.9
NAB/SBE-β-CD	0	20	80.0	81.2	123.1	90.4
	30		79.5	81.1	131.4	96.6
	60		79.7	81.7	124.0	91.1
	90		80.4	82.6	122.6	90.1
	120		77.6	79.4	114.8	84.3
	0	30	80.0	81.2	123.1	91.6
	30		80.0	81.8	107.4	79.9
	60		78.1	80.2	106.1	78.9
	90		77.0	79.2	91.9	68.4
	120		77.5	79.7	80.2	59.7
	NAB/SBE-β-CD COE		82.0	83.6	92.6	66.7

2.2. FT IR spectroscopy

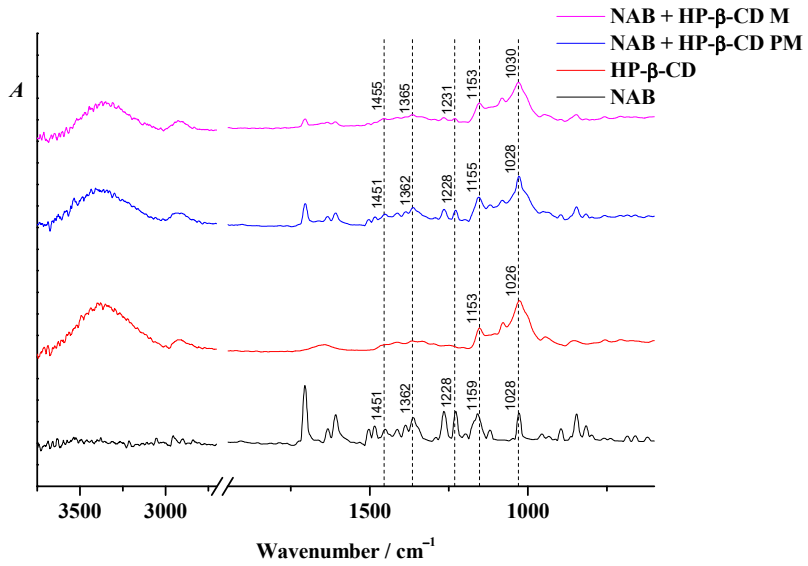


Figure S3. FT-IR ATR spectra of NAB (—), β-CD (—), their physical mixture (PM) (—), and complex (M) prepared by grinding at 20 Hz for 120 min in ZrO_2 jars (—).

Table S4. Assignation of ATR spectra of NAB, β-CD, their physical mixture (PM), and complex (M) prepared by grinding at 20 Hz for 120 min in ZrO_2 jars.

Wavenumber / cm^{-1}				Assignment
NAB	**β-CD**	**NAB+β-CD PM**	**NAB+β-CD M**	
-	3680-3025	3691-3025	3699-3025	ν(OH)
-	2930	2952	2928	ν(CH)
1706	-	1705	1706	ν(C=O)
1608	-	1608	1609	$\nu(C=C)_{aromat}$
1485	-	1484	1484	$\nu(C–C)_{aromat}$
1451	-	1450	1447	δ(HCH)+δ(HCC)
1387	-	1388	1388	δ(HCH)
1362	-	1363	1364	ν(CC)
1265	-	1265	1266	δ(HCC)+τ(HCCC)
1228	-	1228	1230	ν(CC)+τ(HCOC)
1159	-	1156	1154	τ(HCOC)
-	1153	1156	1154	ν(COC)+ν(CC)+δ(COH)
1119	-	1119	1119	ν(CC)+δ(HCC)
-	1078	1079	1079	ν(CO)+ν(CC)+δ(COH)
1028	-	1028	1027	ν(C–O)
-	1027	1028	1027	ν(CC)+δ(COH)+δ(CCH)+δ(CCO)
895	-	895	894	τ(HCCC)
846	-	847	847	τ(HCCC)
816	-	815	814	ν(CC)

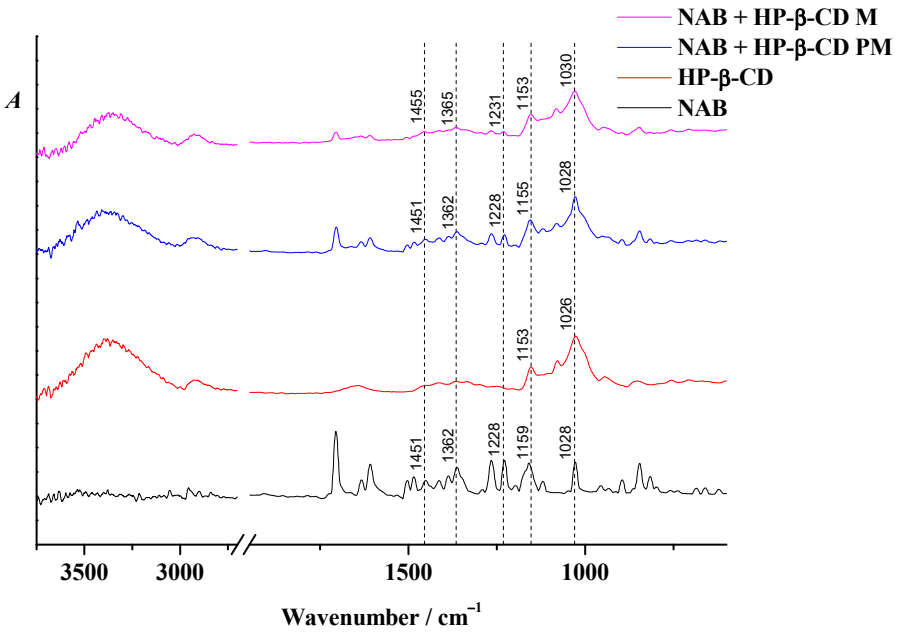


Figure S4. FT-IR ATR spectra of NAB (—), HP-β-CD (—), their physical mixture (PM) (—), and complex (M) prepared by grinding at 30 Hz for 90 min in ZrO_2 jars (—).

Table S5. Assignation of ATR spectra of NAB, HP-β-CD, their physical mixture (PM), and complex (M) prepared by grinding at 30 Hz for 90 min in ZrO_2 jars.

		***Wavenumber* / cm^{-1}**		
NAB	**HP-β-CD**	**NAB+HP-β-CD PM**	**NAB+HP-β-CD M**	**Assignment**
-	3676-3015	3676-3025	3683-3046	ν(OH)
-	2929	2934	2927	ν(CH)
1706	-	1705	1705	ν(C=O)
1608	-	1608	1609	ν(C=C)$_{aromat}$
1485	-	1484	1481sh	ν(C–C)$_{aromat}$
1451	-	1451	1455	δ(HCH)+δ(HCC)
1387	-	1388	1388sh	δ(HCH)
1362	-	1362	1365	ν(CC)
1265	-	1265	1266	δ(HCC)+τ(HCCC)
1228	-	1228	1231	ν(CC)+τ(HCOC)
1159	-	1155	1153	τ(HCOC)
-	1153	1155	1153	ν(COC)+ν(CC)+δ(COC)
1119	-	1119	1119	ν(CC)+δ(HCC)
-	1079	1081	1082	ν(CO)+ν(CC)+δ(OCH)
1028	-	1028	1030	ν(C–O)
-	1026	1028	1030	ν(CC)+ δ(OCH)+δ(CCH)+δ(CCO)
895	-	896	896	τ(HCCC)
846	-	846	847	τ(HCCC)
816	-	816	816	ν(CC)

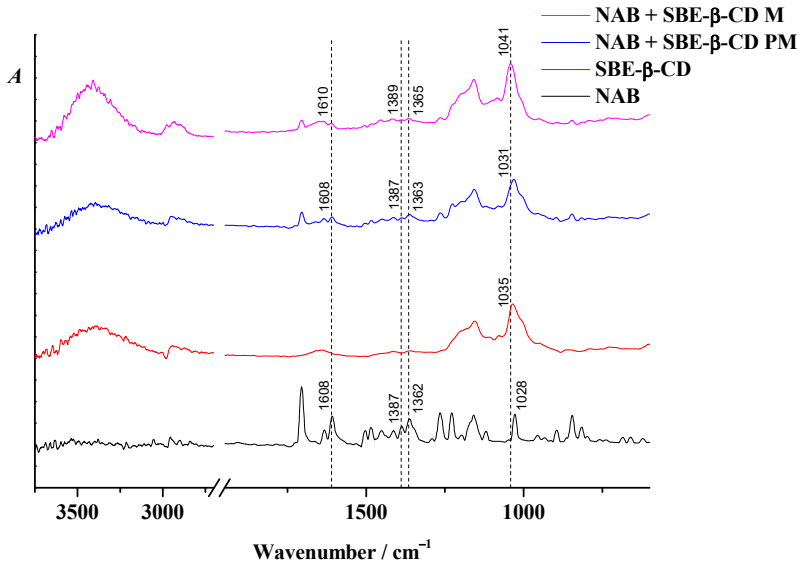


Figure S5. FT-IR ATR spectra of NAB (—), SBE-β-CD (—), their physical mixture (PM) (—), and complex (M) prepared by grinding at 30 Hz for 120 min in ZrO_2 jars (—).

Table S6. Assignation of ATR spectra of NAB, SBE-β-CD, their physical mixture (PM), and complex (M) prepared by grinding at 30 Hz for 90 min in ZrO_2 jars.

NAB	SBE-β-CD	*Wavenumber* / cm^{-1} NAB+SBE-β-CD PM	NAB+SBE-β-CD M	Assignment
-	3724-2982	3709-2987	3694-3012	ν(OH)
-	2943	2949	2933	ν(CH)
1706	-	1706	1705	ν(C=O)
1608	-	1608	1610	ν(C=C)$_{aromat}$
1485	-	1484	1484sh	ν(C–C)$_{aromat}$
1451	-	1448	1455	δ(HCH)+δ(HCC)
1387	-	1387	1389	δ(HCH)
1362	-	1363	1365	ν(CC)
1265	-	1265	1265	δ(HCC)+τ(HCCC)
1228	-	1227	1227sh	ν(CC)+τ(HCOC)
1159	-	1157	1158	τ(HCOC)
-	1155	1157	1158	ν(COC)+ν(CC)+δ(COC)
1119	-	-	-	ν(CC)+δ(HCC)
-	1078	1079	1084	ν(CO)+ν(CC)+δ(OCH)
1028	-	1031	1041	ν(C–O)
-	1035	1031	1041	ν(CC)+ν(SO)+δ(OCH)+δ(CCH)+δ(CCO)
895	-	897	894	τ(HCCC)
846	-	847	847	τ(HCCC)
816	-	816	814	ν(CC)

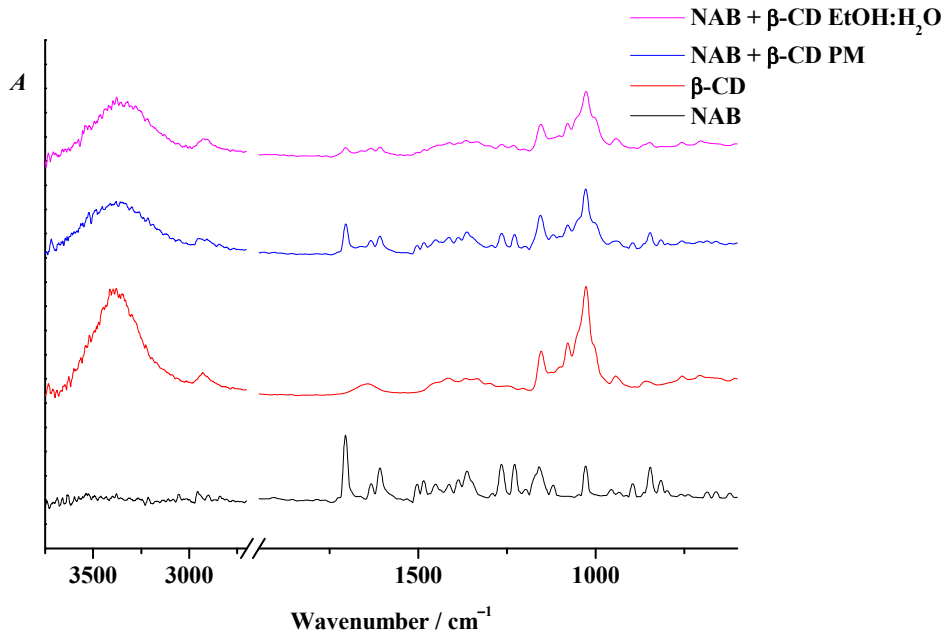


Figure S6. FT-IR ATR spectra of NAB (—), β-CD (—), their physical mixture (PM) (—), and complex (M) prepared by co-evaporation from EtOH:H_2O mixture (—).

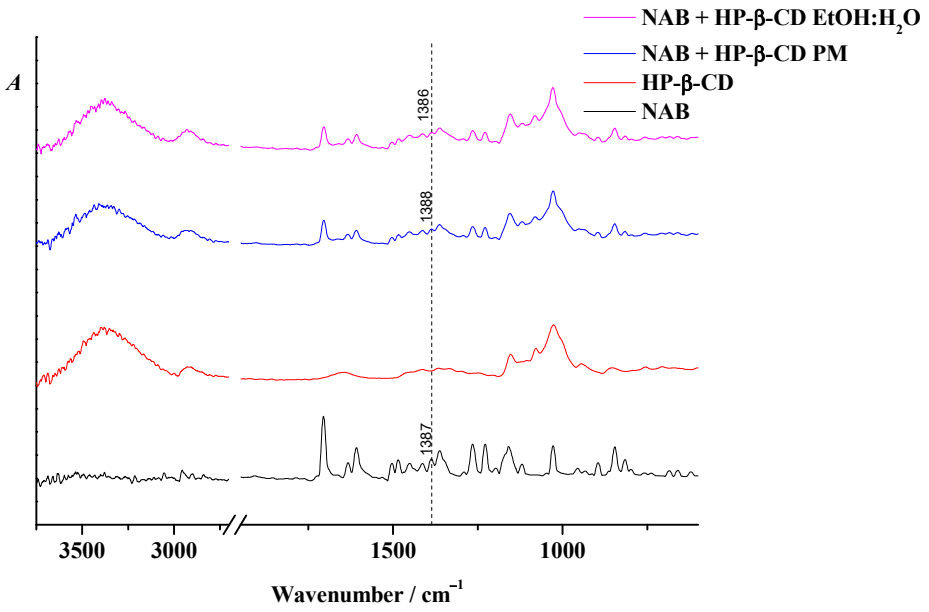


Figure S7. FT-IR ATR spectra of NAB (—), HP-β-CD (—), their physical mixture (PM) (—), and complex (M) prepared by co-evaporation from EtOH:H_2O mixture (—).

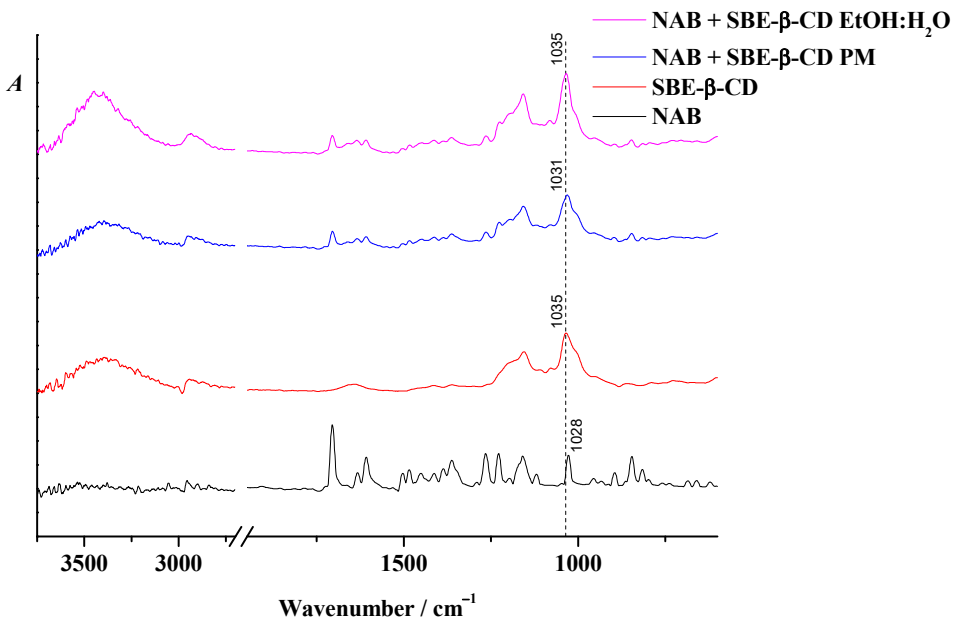


Figure S8. FT-IR ATR spectra of NAB (—), SBE-β-CD (—), their physical mixture (PM) (—), and complex (M) prepared by co-evaporation from EtOH:H_2O mixture (—).

3. Effect of β-cyclodextrins on NAB chemical and photochemical stability

3.1. Hydrolytic degradation

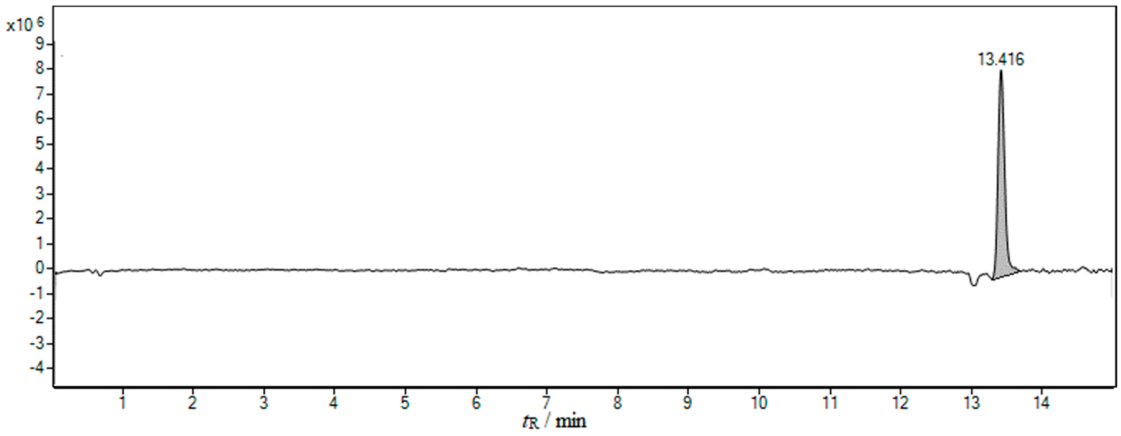


Figure S9. Total ion chromatogram of NAB.

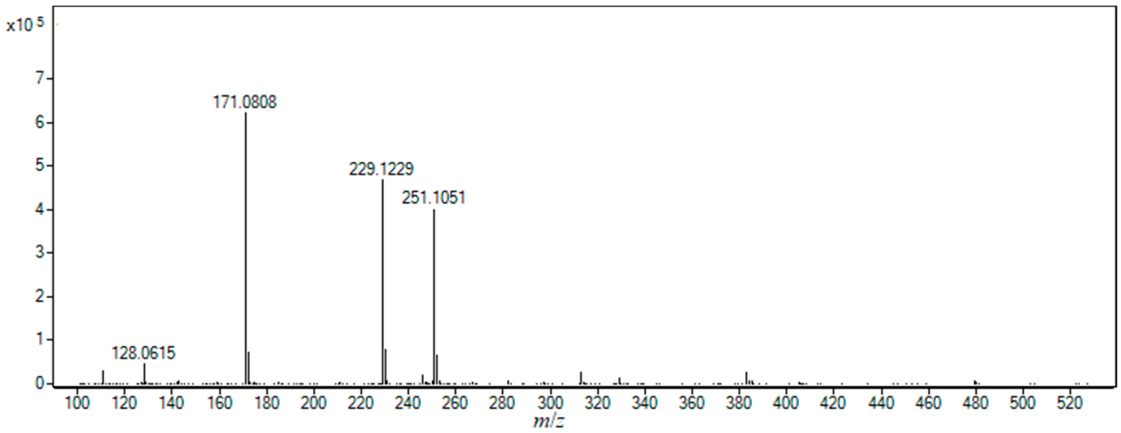


Figure S10. MS spectrum of NAB. (t_R = 13.4 min).

Table S7. Measured and calculated *m*/*z* values, relative intensities, errors and asignation of signals in MS spectrum of NAB (t_R = 13.4 min).

Measured *m*/*z*	Calculated *m*/*z*	Error / ppm	Relative intensity / %	Assignation
479.2190	479.2193	0.63	1.86	$[2M+Na]^+$
251.1051	251.1043	3.38	64.54	$[M+Na]^+$
229.1229	229.1223	2.59	75.46	$[M+H]^+$
171.0808	171.0804	2.10	100	$[M+H–58]^+$
128.0615	128.0621	-4.31	7.69	$[C_{10}H_8]^{\bullet+}$

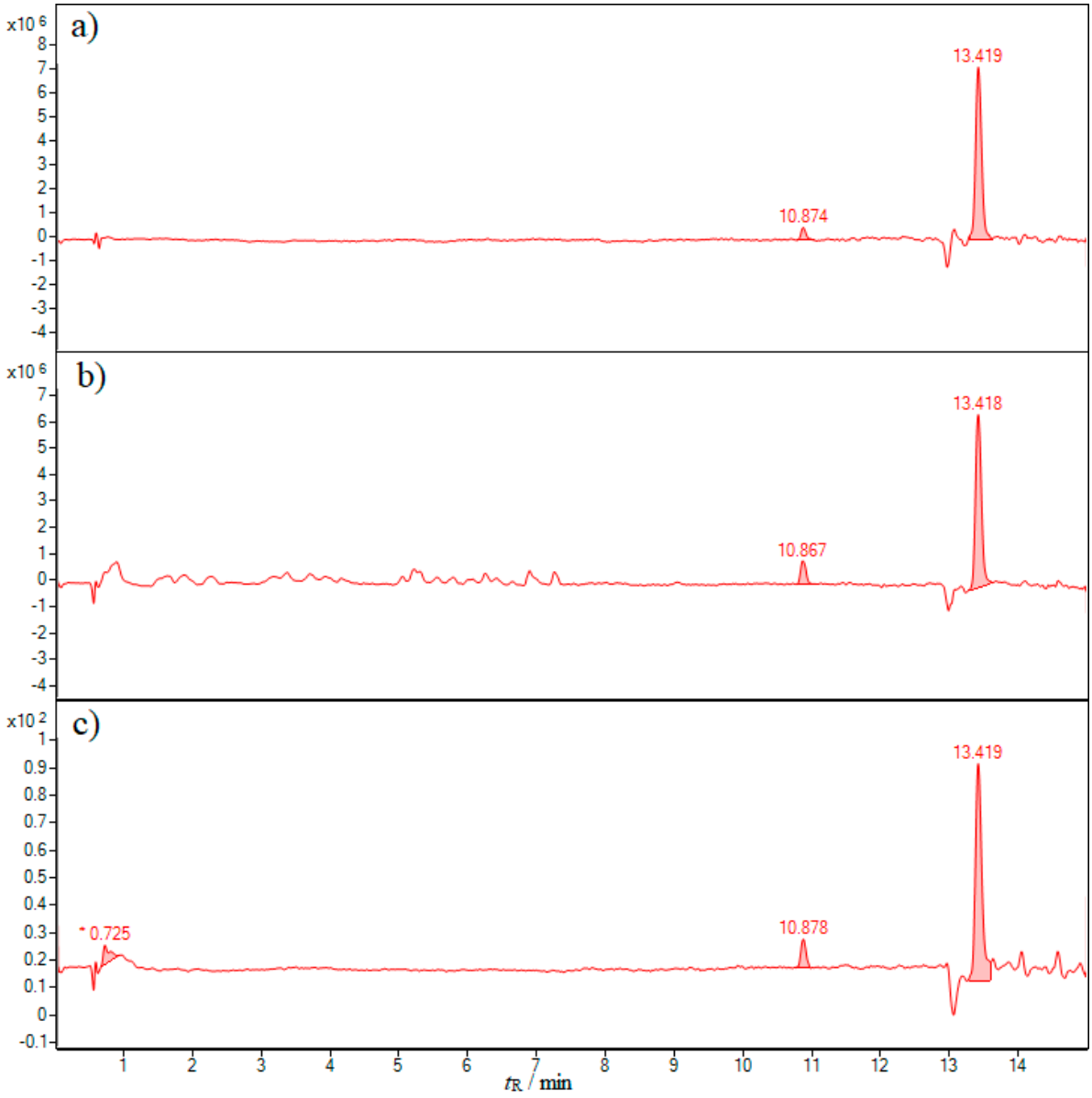


Figure S11. Total ion chromatograms of a) NAB, b) NAB-HP-β-CD, and c) NAB-SBE-β-CD under the hydrolytic degradation in acidic media.

Table S8. MS/MS spectrum of degradation product DP 1 (t_R = 10.9 min) at collision potential of 10 V.

Measured *m/z*	Rel. intensity	Assignation
215,1065	3.27	$[M+H]^+$
157,0640	100	$[C_{11}H_9O]^+$

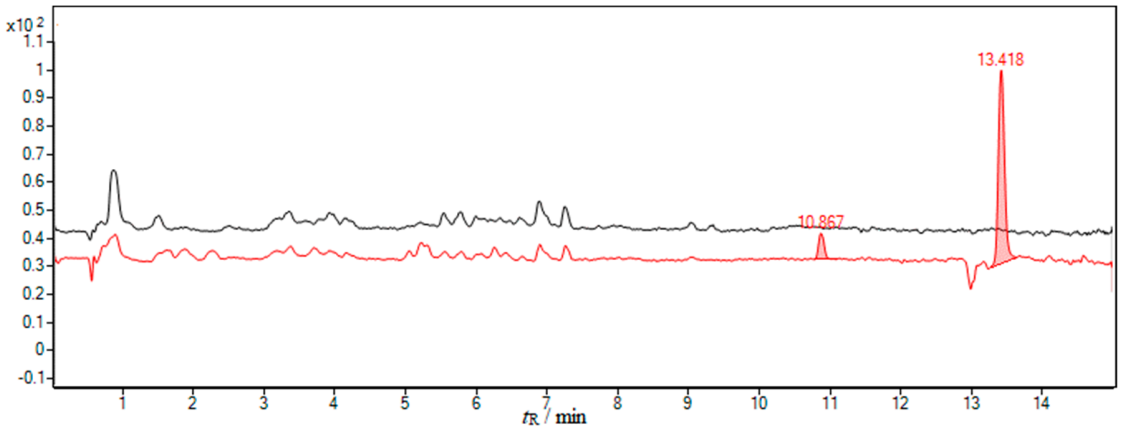


Figure S12. Total ion chromatogram of pure HP-β-CD (—) and NAB:HP-β-CD after the hydrolytic degradation in acidic media (—).

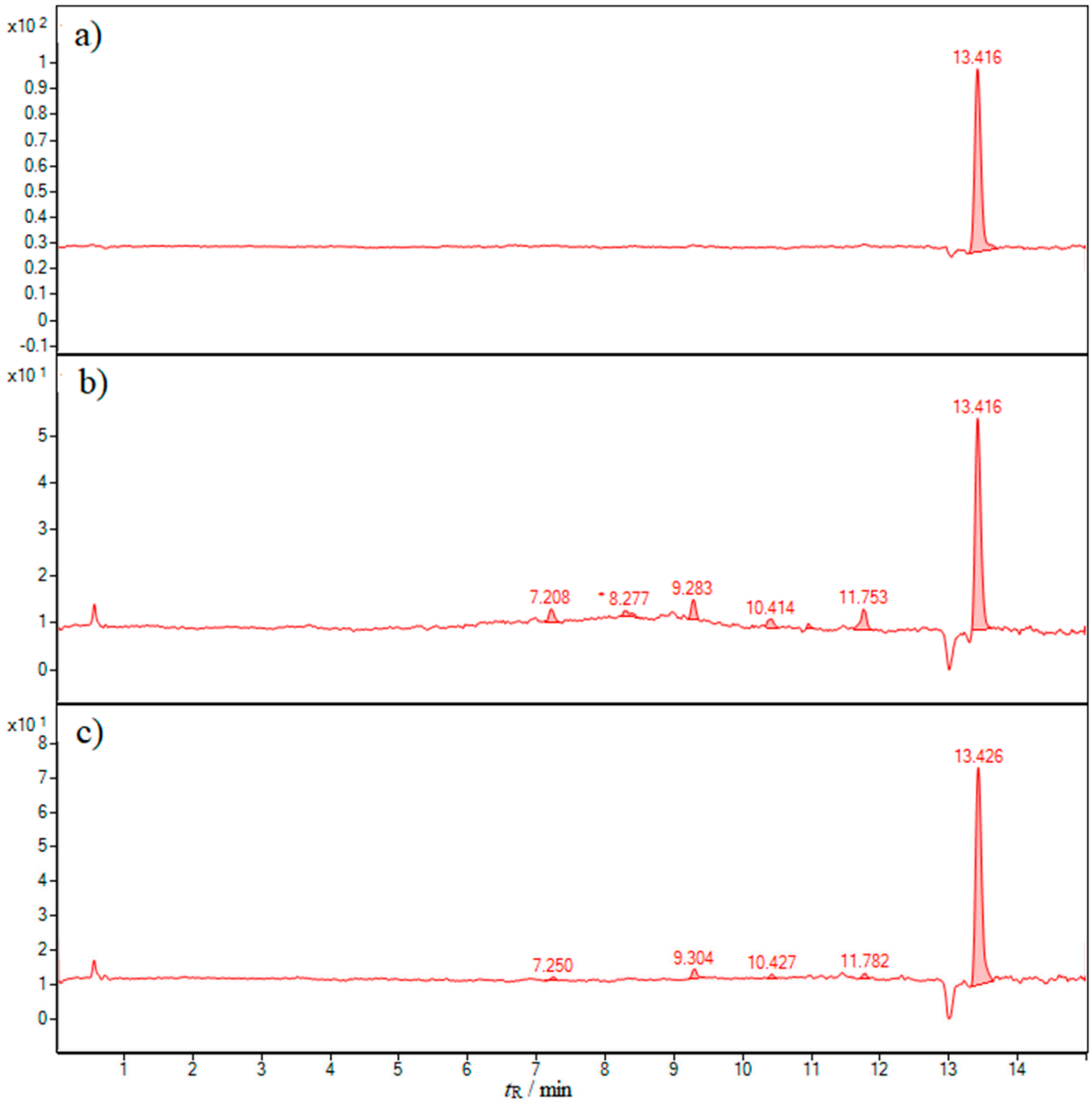


Figure S13. Total ion chromatograms of a) NAB, b) NAB-HP-β-CD, and c) NAB-SBE-β-CD under the oxidative degradation.

Table S9. MS/MS spectrum of degradation product DP 2 (t_R = 7.2 min) at collision potential of 10 V.

Measured *m*/*z*	Rel. intensity / %	Assignation
237.0747	-	$[M+H]^+$
219.0643	**100**	$[C_{12}H_{10}O_4]^+$
161.0221	3.56	$[C_9H_5O_3]^+$

Table S10. MS/MS spectrum of degradation product DP 3 (t_R = 7.2 min) at collision potential of 10 V.

Measured *m*/*z*	Rel. intensity / %	Assignation
293.1023	6.22	$[M+H]^+$
275.0919	33.26	$[C_{15}H_{15}O_5]^+$
261.0754	7.33	$[C_{14}H_{13}O_5]^+$
247.0964	11.30	$[C_{14}H_{15}O_4]^+$
243.0653	**100**	$[C_{14}H_{11}O_4]^+$
233.0807	15.22	$[C_{13}H_{13}O_4]^+$
231.1016	14.07	$[C_{14}H_{15}O_3]^+$
219.1015	40.98	$[C_{13}H_{15}O_3]^+$
215.0700	8.14	$[C_{13}H_{11}O_3]^+$

Table S11. MS/MS spectrum of degradation product DP 4 (t_R = 8.8 min) at collision potential of 10 V.

Measured *m*/*z*	Rel. intensity / %	Assignation
251.0902	-	$[M+H]^+$
233.0798	57.96	$[C_{13}H_{13}O_4]^+$
219.0645	**100**	$[C_{12}H_{11}O_4]^+$

Table S12. MS/MS spectrum of degradation product DP 5 (t_R = 9.0 min) at collision potential of 10 V.

Measured *m*/*z*	Rel. intensity / %	Assignation
263.0902	7.78	$[M+H]^+$
235.0957	1.59	$[C_{14}H_{12}O_5]^+$
203.0686	**100**	$[C_{12}H_{11}O_3]^+$

Table S13. MS/MS spectrum of degradation product DP 6 (t_R = 9.3 min) at collision potential of 10 V.

Measured *m*/*z*	Rel. intensity / %	Assignation
277.1054	11.30	$[M+H]^+$
245.0798	3.53	$[C_{14}H_{13}O_4]^+$
227.0689	4.09	$[C_{14}H_{11}O_3]^+$
203.0695	**100**	$[C_{12}H_{11}O_3]^+$

Table S14. MS/MS spectrum of degradation product DP 7 (t_R = 9.5 min) at collision potential of 10 V.

Measured *m*/*z*	Rel. intensity / %	Assignation
217.0854	**100**	$[M+H]^+$
159.0432	5.54	$[C_{10}H_7O_2]^+$

Table S15. MS/MS spectrum of degradation product DP 8 (t_R = 10.4 min) at collision potential of 10 V.

Measured *m*/*z*	Rel. intensity / %	Assignation
261.1106	**100**	$[M+H]^+$
229.0848	68.99	$[C_{14}H_{13}O_3]^+$
203.0695	56.17	$[C_{12}H_{11}O_3]^+$
201.0900	52.91	$[C_{13}H_{13}O_2]^+$
171.0429	17.17	$[C_{11}H_7O_2]^+$

Table S16. MS/MS spectrum of degradation product DP 9 (t_R = 11.0 min) at collision potential of 10 V.

Measured *m*/*z*	Rel. intensity / %	Assignation
245.0773	10.40	$[M+H]^+$
227.0688	51.69	$[C_{14}H_{11}O_3]^+$
209.0576	14.94	-
201.0897	4.83	$[C_{13}H_{13}O_2]^+$
199.0744	19.76	$[C_{13}H_{11}O_2]^+$
185.0601	16.02	$[C_{12}H_9O_2]^+$
183.0792	**100**	$[C_{13}H_{11}O]^+$

Table S17. MS/MS spectrum of degradation product DP 10 (t_R = 11.8 min) at collision potential of 10 V.

Measured *m*/*z*	Rel. intensity / %	Assignation
259.0949	15.79	$[M+H]^+$
241.0846	55.49	$[C_{14}H_{11}O_3]^+$
227.0691	15.87	$[C_{14}H_{11}O_2]^+$
209.0585	71.28	$[C_{13}H_{11}O_2]^+$
199.0741	10.48	$[C_{14}H_{13}O]^+$
197.0953	**100**	$[C_{13}H_{11}O]^+$

Table S18. MS/MS spectrum of degradation product DP 11 (t_R = 11.8 min) at collision potential of 10 V.

Measured *m*/*z*	**Rel. intensity / %**	**Assignation**
291.0857	**100**	$[M+H]^+$
259.0595	54.86	$[C_{14}H_{11}O_5]^+$
231.0643	4.72	$[C_{13}H_{11}O_4]^+$
203.0697	10.16	$[C_{12}H_{11}O_3]^+$

3.2. Photostability study

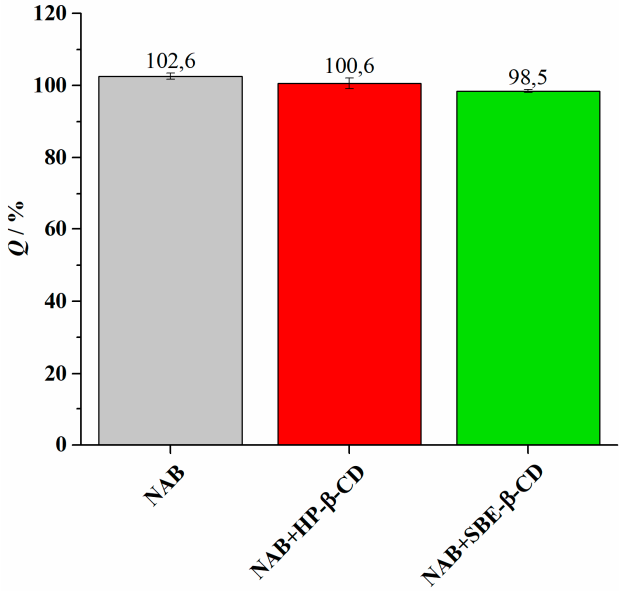


Figure S14. NAB content in sample of pure NAB and in NAB-HP-β-CD and NAB-SBE-β-CD samples prepared by grinding subjected to photostability studies

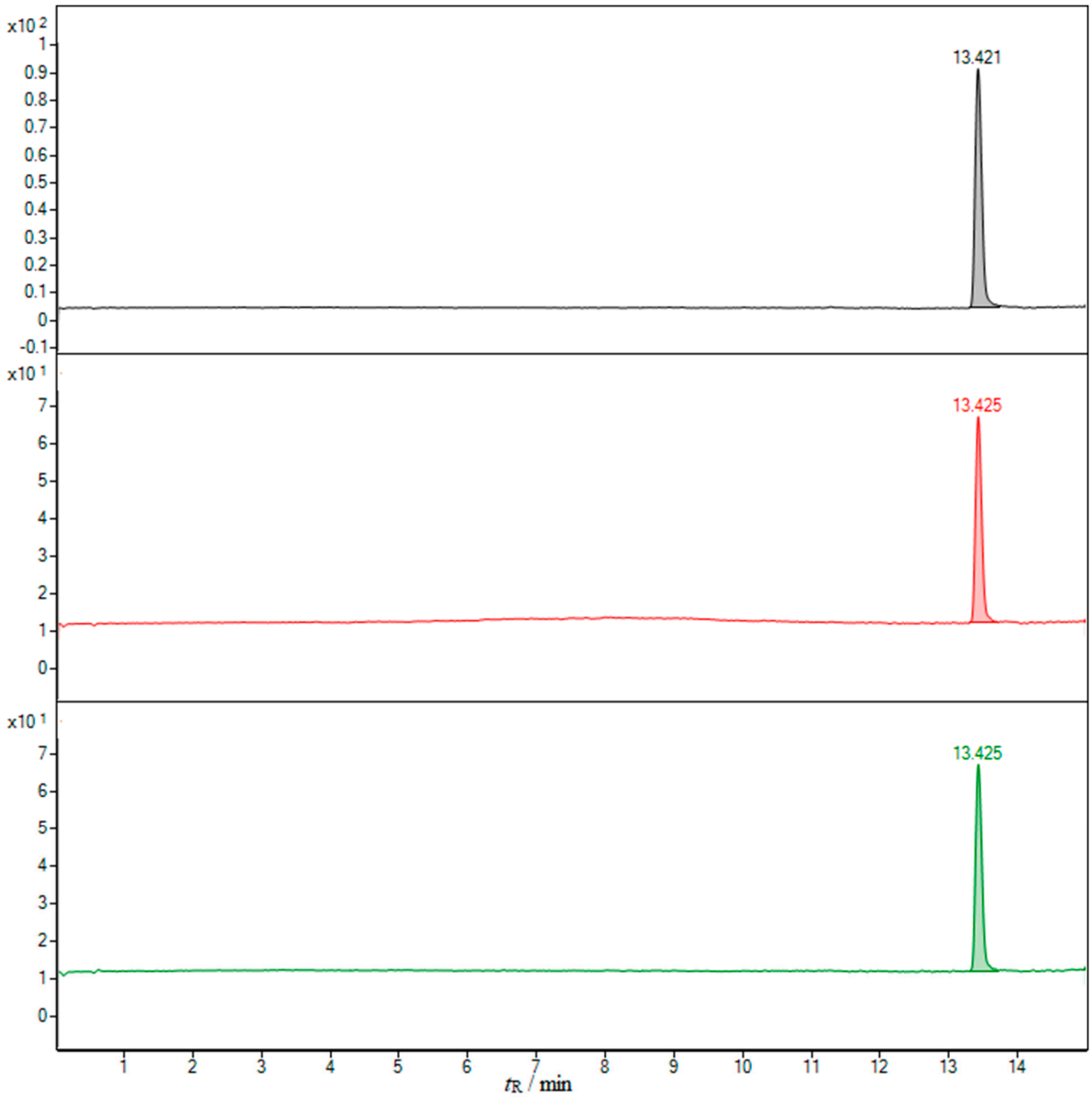


Figure S15. Total ion chromatograms of NAB (—), NAB-HP-β-CD (—), and NAB-SBE-β-CD (—) samples after subjecting to photostability studies.

3.3. Long-term stability study

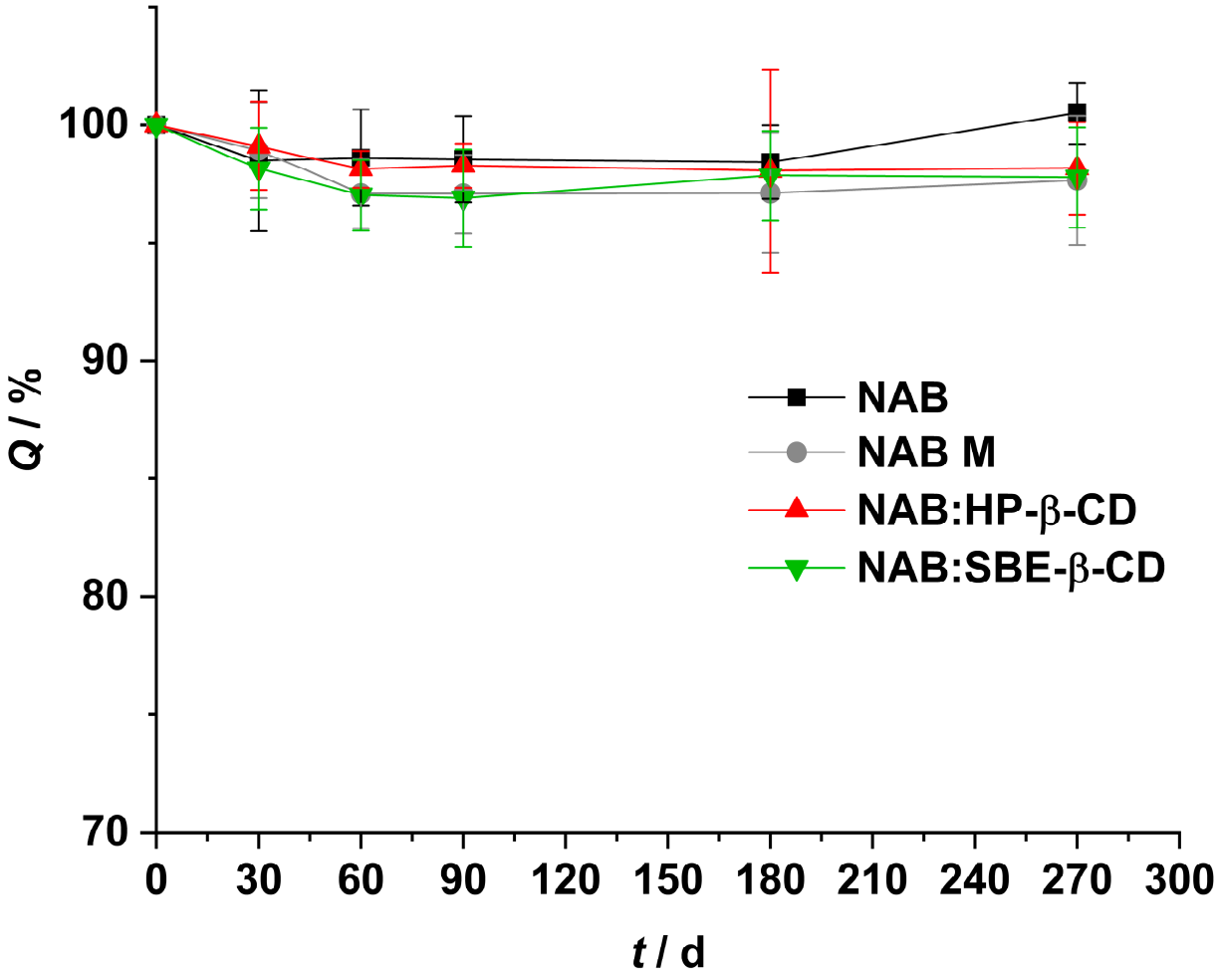


Figure S16. NAB content in samples of pure NAB, grinded NAB and in NAB-HP-β-CD and NAB-SBE-β-CD samples prepared by grinding during the long-term stability studies for 9 months.

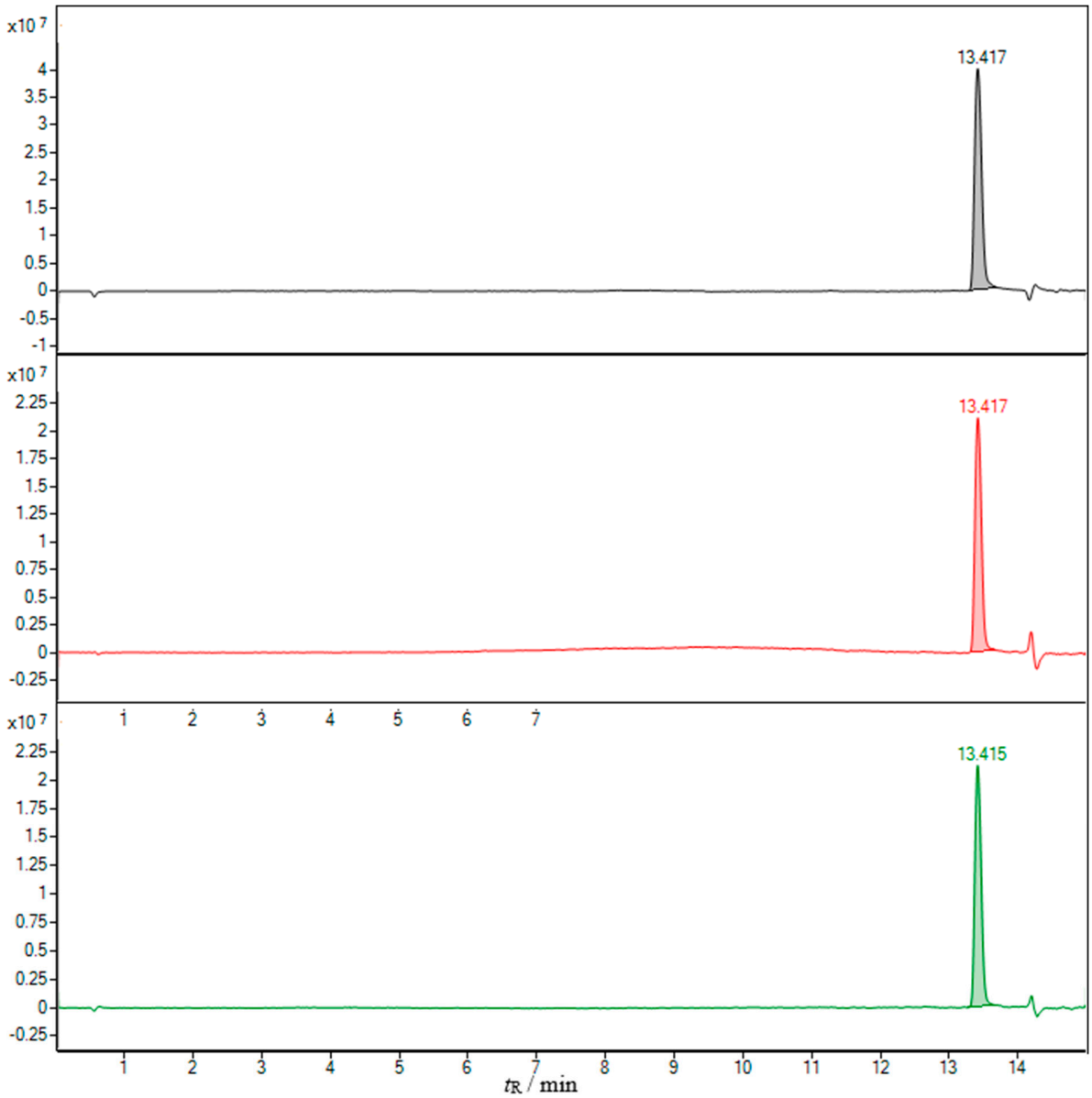


Figure S17. Total ion chromatograms of NAB (—), NAB-HP-β-CD (—), and NAB-SBE-β-CD (—) samples after the period of 9 months of long-term stability studies.